The *Evf-2* noncoding RNA is transcribed from the Dlx-5/6 ultraconserved region and functions as a Dlx-2 transcriptional coactivator

Jianchi Feng, Chunming Bi, Brian S. Clark, Rina Mady, Palak Shah, and Jhumku D. Kohtz[1]

Program in Neurobiology and Department of Pediatrics, Children's Memorial Hospital and Feinberg School of Medicine, Northwestern University, Chicago, Illinois 60614, USA

The identification of ultraconserved noncoding sequences in vertebrates has been associated with developmental regulators and DNA-binding proteins. One of the first of these was identified in the intergenic region between the *Dlx-5* and *Dlx-6* genes, members of the Dlx/*dll* homeodomain-containing protein family. In previous experiments, we showed that Sonic hedgehog treatment of forebrain neural explants results in the activation of *Dlx-2* and the novel noncoding RNA (ncRNA), *Evf-1*. In this report, we show that the *Dlx-5/6* ultraconserved region is transcribed to generate an alternatively spliced form of *Evf-1*, the ncRNA *Evf-2*. *Evf-2* specifically cooperates with Dlx-2 to increase the transcriptional activity of the Dlx-5/6 enhancer in a target and homeodomain-specific manner. A stable complex containing the *Evf-2* ncRNA and the Dlx-2 protein forms in vivo, suggesting that the *Evf-2* ncRNA activates transcriptional activity by directly influencing Dlx-2 activity. These experiments identify a novel mechanism whereby transcription is controlled by the cooperative actions of an ncRNA and a homeodomain protein. The possibility that a subset of vertebrate ultraconserved regions may function at both the DNA and RNA level to control key developmental regulators may explain why ultraconserved sequences exhibit 90% or more conservation even after 450 million years of vertebrate evolution.

[*Keywords*: Noncoding RNA; homeodomain transcription factors; forebrain development; Dlx gene regulation; ultraconserved region]

Received January 31, 2006; revised version accepted March 22, 2006.

In the past few years, there has been increasing interest in how ncRNAs function in gene regulation, dosage compensation, and imprinting. Several reviews have emphasized that the role of ncRNAs in different cellular processes has been largely underestimated (Kelley and Kuroda 2000; Eddy 2001, 2002; Erdmann et al. 2001; Akhtar 2003). What is most surprising is that even in a system as well studied as *Escherichia coli*, the role of small ncRNAs are only now beginning to be understood.

In addition to a variety of functions in the nucleus, ncRNAs can function in the cytoplasm to regulate mRNA stability, translation efficiency, and protein transport. The class of ncRNAs includes the well-known groups: ribosomal RNA (rRNA), small nuclear RNA (snRNA), and transfer RNA (tRNA). However, recent discoveries have added several new types of RNAs to this list, including microRNA (miRNA, putative translational regulatory gene family), small interfering RNA (siRNA), and small nucleolar RNA (snoRNA, involved in rRNA modification). Among this growing list of ncRNAs is a group associated with human disease: DGCR5, breakpoint region in DiGeorge syndrome (Sutherland et al. 1996); K*vLQTA-AS*, implicated in Beckwith-Wiedeman syndrome (Lee et al. 1999); SCA8, spinocerebellar ataxia type 8 (Nemes et al. 2000); and *CMPD*-associated RNA, Campomelic dysplasia (Ninomiya et al. 1996). As the number of non-mRNA functional RNAs increases, there is likely to be more acceptance that such RNAs may play important regulatory roles with their alterations resulting in human diseases.

Although nuclear ncRNAs can function in gene regulation, dosage compensation, and imprinting, specific *trans*-acting effects of developmentally regulated ncRNAs on transcription have not been reported. In a screen for genes differentially expressed in the embryonic dorsal and ventral telencephalon, we isolated *Evf-1* (Kohtz et al. 1998), a novel downstream target of the patterning protein Sonic hedgehog (for review, see Ingham and McMahon 2001). More recently, we showed

[1]**Corresponding author.**
E-MAIL j-kohtz@northwestern.edu; FAX (773) 755-6344.
Article published online ahead of print. Article and publication date are online at http://www.genesdev.org/cgi/doi/10.1101/gad.1416106.

that *Evf-1* is a developmentally regulated, 2.7-kb polyadenylated ncRNA, transcribed upstream of the mouse *Dlx-6* gene (Kohtz and Fishell 2004). Vertebrate Dlx genes are part of a homeodomain protein family related to the *Drosophila* Distalless gene (*dll*) (for review, see Panganiban and Rubenstein 2002). Genetic deletion of *Dlx* genes in mice demonstrates their critical role in neuronal differentiation and migration, as well as craniofacial and limb patterning during development (Anderson et al. 1997a,b; Acampora et al. 1999; Depew et al. 1999; Robledo et al. 2002). Most recently, loss of *Dlx-1* has been associated with specific neuronal loss and epilepsy (Cobos et al. 2005). The *Dlx* genes are expressed in bigene clusters, and conserved intergenic enhancers have been identified for the *Dlx-5/6* and *Dlx-1/2* loci (Ghanem et al. 2003; Zerucha et al. 2000). It has also been shown that Dlx-2 (Porteus et al. 1991) binds sequences in the conserved *Dlx-5/6* intergenic region, both by gel shift and CHIP analyses (Zerucha et al. 2000; Zhou et al. 2004). *Evf-1* expression closely resembles Dlx-6 sense RNA and previously identified antisense RNA (Liu et al. 1997) expression in the ventral forebrain and branchial arches (BAs) (Kohtz and Fishell 2004). The close association between *Evf-1* and Dlx-6 expression led us to further characterize transcripts within the Dlx-5 and 6 loci.

In this report, we show that *Evf-2,* an alternatively spliced form of *Evf-1*, is transcribed from ei, one of the two Dlx-5/6 conserved intergenic regions identified previously by Zerucha et al. (2000). Recent reports suggest that ei is one of several hundred ultraconserved sequences located close to other key developmental regulators and DNA-binding proteins (Santini et al. 2003; Spitz et al. 2003; Bejerano et al. 2004; Boffelli et al. 2004; Sabarinadh et al. 2004; Sandelin et al. 2004; Woolfe et al. 2005). The function of these ultraconserved regions is presently not known. We show here that transcription of the Dlx-5/6 ei is conserved in vertebrates, and that the ultraconserved region of *Evf-2* cooperates with the homeodomain protein Dlx-2 to increase the activity of the Dlx-5/6 enhancer in a target and homeodomain-specific manner. These studies suggest that developmentally regulated ncRNAs may function in *trans* to regulate the transcriptional activity of homeodomain proteins. Therefore, an additional level of complexity in the control of homeodomain protein activity may occur through RNAs transcribed from ultraconserved regions. We propose that *Evf-2* falls into a novel class of transcription regulating, ultraconserved ncRNAs (trucRNAs).

Results

The Evf-2 *ncRNA transcript overlaps with the ultraconserved Dlx-5/6 intergenic enhancer*

Conservation of the Dlx-5/6 intergenic enhancer elements ei and eii in humans, rodents, and zebrafish was shown previously (Fig. 1a,b; Zerucha et al. 2000). Inclusion of chickens in this alignment shows that ei, but not eii is also conserved in chickens (Fig. 1a). This classifies the Dlx-5/6 ei sequence as one of many ultraconserved regions found in the vertebrate genome. Analysis of transcripts by isolation from a cDNA library (rat), RT–PCR (zebrafish and chicken), or expressed sequence tag (EST) databases (human and mouse) shows that ei transcription is conserved in vertebrates (Fig. 1a). We isolated a full-length cDNA containing ei sequences from a rat embryonic day 15.5 (E15.5) brain library, and found it to be a 3.8-kb alternatively spliced form of *Evf-1*, an ncRNA previously identified as a downstream target of Shh signaling in the rat embryonic forebrain (Kohtz et al. 1998; Faedo et al. 2004; Kohtz and Fishell 2004). We named this 3.8-kb, ei-containing alternatively spliced form of *Evf-1*, *Evf-2*.

The genomic organization of the four mouse Evf exons (Fig. 1b) was determined based on Evf-1 and Evf-2 rat cDNA sequences, the mouse EST and genomic databases, as well as analysis of transcripts obtained by RT–PCR from mouse embryonic brain (data not shown). *Evf-1* and *Evf-2* transcripts result from alternative transcription initiation, alternative splicing of exon 3, and alternative polyadenylation. The Evf-2 5′ transcription initiation site was mapped by RNase protection, immediately 3′ to eii (data not shown). Exon 2 contains the ultraconserved Dlx-5/6 enhancer ei (Zerucha et al. 2000), therefore, *Evf-2* sequences in red (116–459) are encoded by this ultraconserved Dlx-5/6 enhancer ei. Both Evf-1 and Evf-2 mouse cDNAs can be detected by PCR analysis of mouse embryonic ventral forebrain cDNAs (data not shown). Sequence comparisons of the Evf-1 and Evf-2 cDNA sequences reveal unique 5′ and 3′ ends and a 2561-base-pair (bp) region of identity (blue region, Fig. 1c). Northern analysis (Fig. 1d) shows that *Evf-1* and *Evf-2* RNAs are present in rat ventral telencephalic total and polyadenylated RNA fractions, but not in dorsal RNA fractions. A large (7.5-kb) nonpolyadenylated form recognized by both *Evf-1* and *Evf-2* probes is present in the total RNA fraction and absent from the poly A-containing fraction. The *Evf-2*-specific probe identifies a smaller (500-bp) species. RNase protection (Fig. 1e) using a probe spanning the Evf 2/Evf common region junction probe detects a 440-bp protected fragment, the expected size for *Evf-2*, and a 200-bp fragment, the expected size for *Evf-1*. In situ hybridization using *Evf-2* 5′-specific probes reveals a ventral forebrain expression pattern indistinguishable from *Evf-1* (Kohtz et al. 1998; Kohtz and Fishell 2004) and similar to the Dlx-5/6 expression pattern (Fig. 1f,g; Liu et al. 1997; Eisenstat et al. 1999; Zerucha et al. 2000). *Evf-2*, like *Evf-1*, is expressed by immature neurons (Kohtz and Fishell 2004) as they exit the ventricular zone and enter the post-mitotic layer (data not shown). In the E11.5 rat ventral telencephalon, *Evf-2* transcripts localize in dense regions within nuclei stained with DAPI (Fig. 1f). Figure 1g shows the overlapping expression of the Dlx homeodomain members Dlx-2, Dlx-5, and Dlx-6 with Evf-2 and Shh. Whereas Shh expression is limited to the medial ganglionic eminence (MGE), Evfs and Dlxs are found in both the MGE and lateral ganglionic eminence (LGE). As might be predicted from their overlapping genomic organization, the control of Evf-1/2 and Dlx-5/6 expression in the ventral forebrain is closely linked.

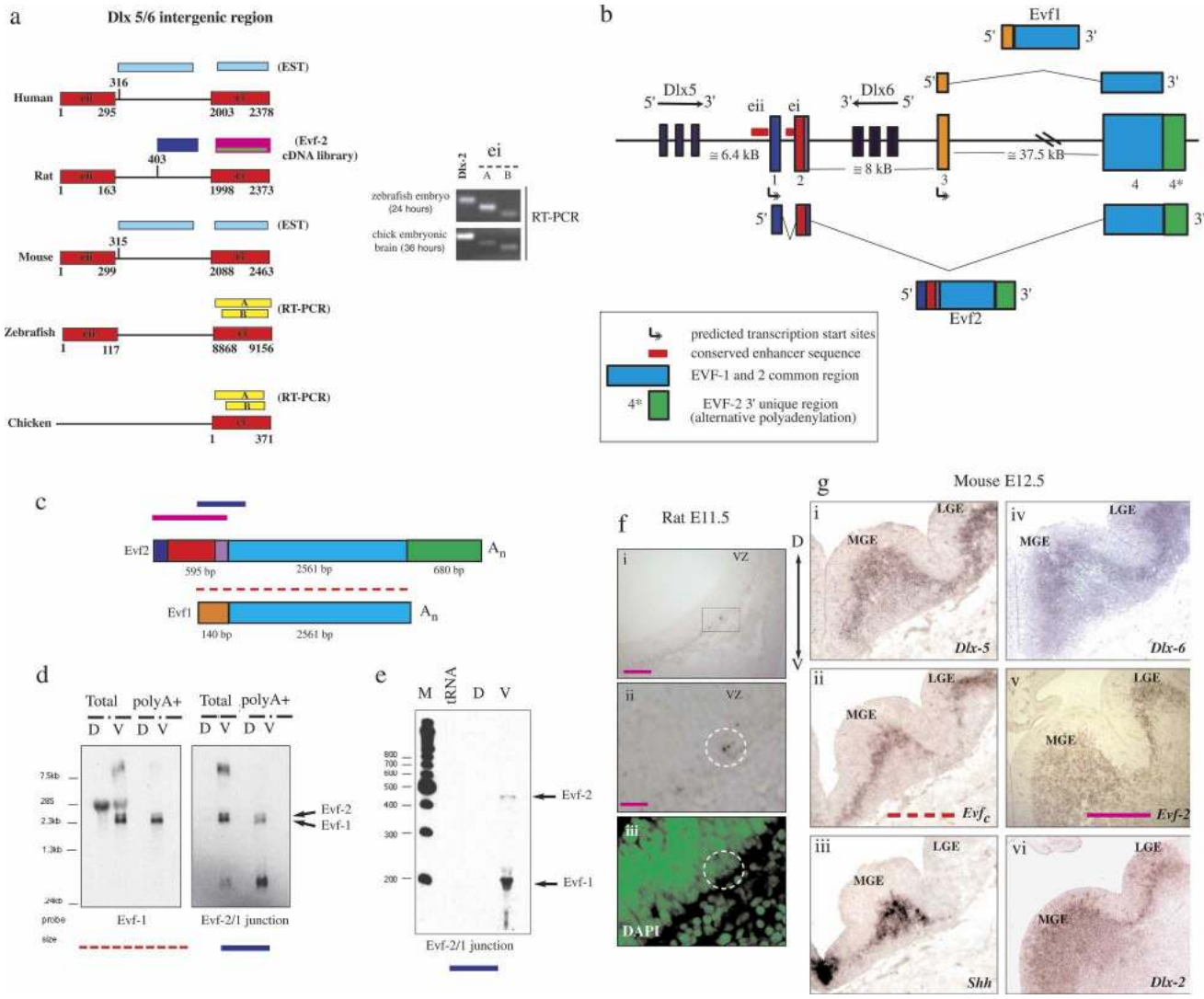

Figure 1. Identification of Evf-2 transcripts. (*a*) The ultraconserved Dlx-5/6 intergenic enhancer ei is transcribed in vertebrates. Human and mouse ESTs were found in the database (sky blue). ei-containing ESTs were not found in the zebrafish and chick databases. The *right* panel shows that two different primer sets (A and B) detect ei-containing transcripts in cDNAs made from zebrafish embryos or chick embryonic brains. (*b*) Genomic organization of the mouse Evf gene. *Evf-1* and *Evf-2* result from alternate transcription initiation, alternative splicing of exon 3, and alternative polyadenylation. Exon 2, included in *Evf-2* but absent from *Evf-1*, is partly encoded by the conserved intergenic enhancer ei (red). (*c*) Schematic representation of *Evf-1* and *Evf-2*. Common regions are shown in blue. *Evf-2* nucleotides 116–459 are encoded by the conserved intergenic enhancer, ei (red). Antisense RNA probes (shown as pink, blue, and red dashed lines) spanning different regions of *Evf-1* and *Evf-2* were used for Northern, RNase protection, and in situ hybridizations, as indicated. (*d*) Northern analysis of total and polyadenylated RNAs isolated from rat E13.5 embryonic telencephalon, using probes generated against *Evf-1* and *Evf-2* (as indicated in *c*). (D) Dorsal; (V) ventral. The full-length *Evf-1* probe detects the 28S rRNA in total RNAs from both dorsal and ventral RNAs, showing that the absence of Evfs in D RNAs is not due to degradation. (*e*) RNase protection. A 450-nt probe spanning the Evf 2/common region junction (blue) detects RNase-resistant bands in ventral (V) but not in dorsal (D) rat E13.5 embryonic telencephalic RNAs or tRNA. (*f*, panels *i*,*ii*) Section in situ hybridization of tissues from rat ventral forebrain at E11.5 using the 5′specific *Evf-2* probe (pink). (Panel *iii*) Dense *Evf-2* staining colocalizes with the nuclear stain DAPI. (*g*) Section in situ hybridization of mouse ventral forebrain at E12.5 using the following antisense probes: Dlx-5 (panel *i*), Evf (1 + common region) (panel *ii*), Shh (panel *iii*), Dlx-6 (panel *iv*), Evf-2 (panel *v*), and Dlx-2 (panel *vi*). (VZ) Ventricular zone; (LGE) lateral ganglionic eminence; (MGE) medial ganglionic eminence; (D) dorsal; (V) ventral. The full-length rat Evf-1 cDNA sequence is available on GenBank (accession no. AY518691).

Although *Evf-1* and *Evf-2* exhibit a high degree (86%–93%) of conservation between rat and mouse sequences in their 5′ and 3′ regions, a compilation of transcripts found in human, rat, mouse, zebrafish, and chicken shows that only transcription from exon 2 is conserved (Fig. 1a). Such conservation of Evf exon 2-encoded transcripts suggests that *Evf-2* may be the functionally significant form. Similar to *Evf-1*, *Evf-2* does not contain

conserved ORFs >200 bp, supporting that both are noncoding. However, the *Evf-2* transcriptionally functional region (defined below) potentially encodes one 19-amino-acid peptide. Although we have not ruled out the possibility that this peptide may be produced, the intranuclear colocalization of the *Evf-2* ncRNA with Dlx-2 (shown below), strongly supports that *Evf-2* RNA is functional.

Shh induces the expression of Evf-2, *Dlx-2, Dlx-5, and Dlx-6 in vivo*

Evf-1 was shown previously to be a downstream target of Shh in embryonic forebrain neural explants in vitro (Kohtz et al. 1998). We next asked whether *Evf-2* is also a downstream target of Shh. In order to determine this, we injected viruses expressing Shh into mouse E9.5 embryonic forebrain, a technique that had demonstrated previously that Shh activates Dlx-2 gene expression in the dorsal telencephalon in vivo (Gaiano et al. 1999; Kohtz et al. 2001). Cell lysates made after pwtShhCLE viral infection express the Shh protein, whereas pCLE virally infected cells do not (Fig. 2a,b). Figure 2c shows how ultrasound back-scatter microscope (UBM) guidance allows in utero injections of the E9.5 mouse brain (Olsson et al. 1997). At E12.5, 3 d after viral injection, serial sections are probed for *Dlx-2, Dlx-5, Dlx-6, Evf-2*, or Evf_c expression in virally infected clusters identified by alkaline phosphatase substrate staining (Fig. 2d,e,o,p). pCLE-infected clusters (Fig. 2f–h) and the dorsal region of littermate controls (Fig. 2k–n) do not express *Dlx*s or *Evf*s at this time in development. pwtShhCLE infection

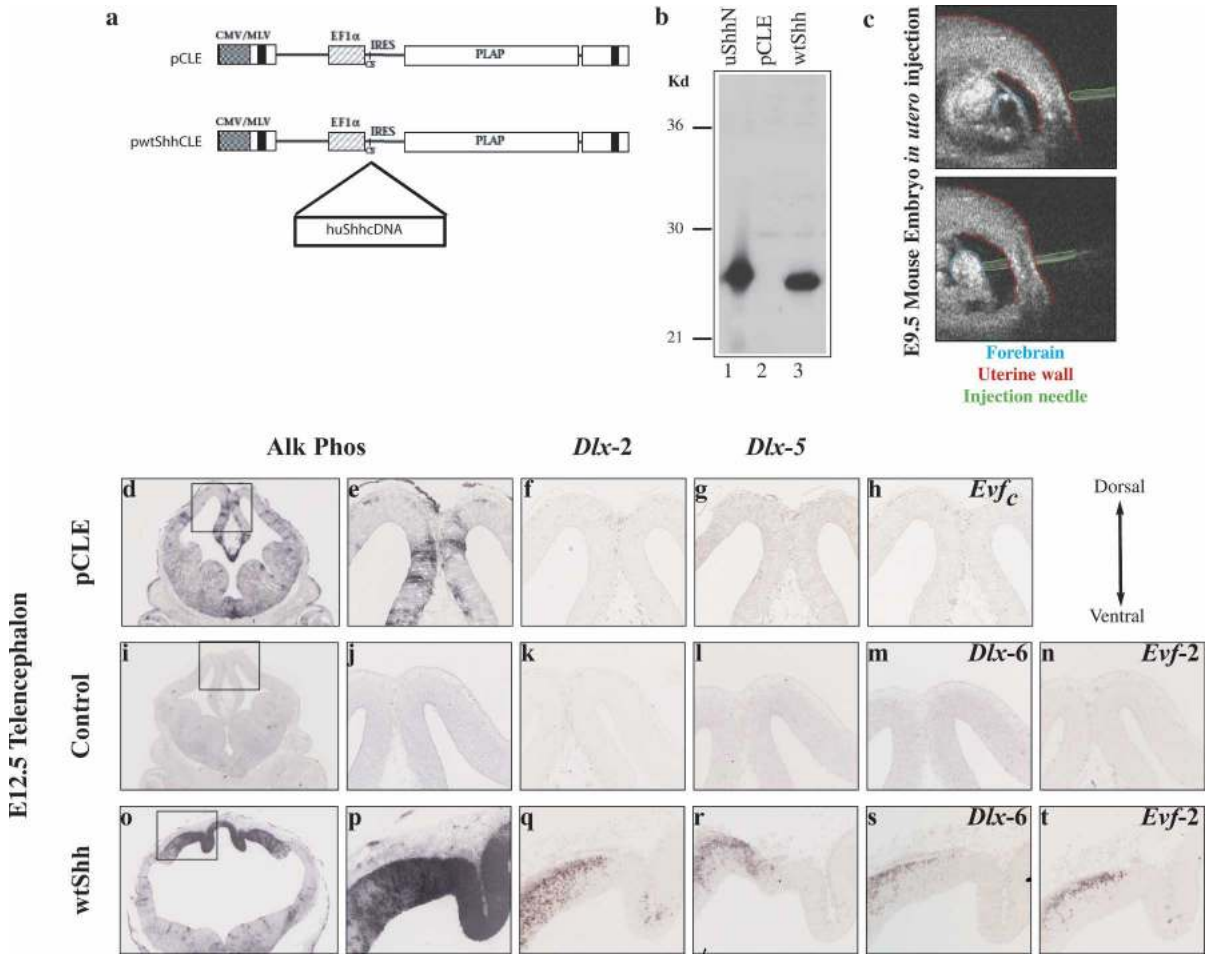

Figure 2. Sonic hedgehog induces the expression of Evf, Dlx-2, and Dlx-5 in vivo. (*a*) Diagram of retroviral backbone used to express the human sonic hedgehog protein (pwtShhCLE) or control (pCLE). Alkaline phosphatase is bicistronic with the Shh cDNA, allowing detection of virally infected cells. (*b*) Lysates of C17 cells infected with wtShh virus (lane *3*), pCLE control virus (lane *2*), or 7 ng of purified recombinant-unmodified Shh (lane *1*, uShhN) were Western-blotted and probed with anti-Shh antibody (Santa Cruz Biotechnology). (*c*) In utero UBM-guided entry of viruses into E9.5 mouse forebrain. Sections of E12.5 mouse brains 3 d after infection with control pCLE virus (*d–h*), littermate control (*i–n*), or wtShh virus (*o–t*). (*d,e*) pCLE virus-infected clusters. (*o,p*) wtshh-infected viral clusters visualized by alkaline phosphatase staining in the dorsal midline of the telencephalon. (*i,j*) Uninfected littermate control does not contain alkaline phosphatase-expressing clusters of cells. In situ hybridization of adjacent sections probed for ectopic expression of ventral genes Dlx-2 (*f,k,q*), Dlx-5 (*g,l,r*), Evf_c (*h*), Dlx-6 (*m,s*), and Evf-2 (*n,t*). Orientation of the section is indicated in the *top right* box.

results in the ectopic activation of Dlx-2, Dlx-5, Dlx-6, and Evf-2, demonstrating that Shh signaling activates all four genes in the same region in the brain (Fig. 2q–t).

Evf-2 *cooperates with Dlx-2 to activate the Dlx-5/6 enhancer*

The close relationship between *Evf-2* and the Dlx-5/6 enhancer, the presence of ei sequences in the 5′ unique region of *Evf-2,* and the evolutionary conservation of Evf exon 2-containing transcripts led us to ask whether *Evf-2* may function in *trans* by regulating the transcriptional activity of the Dlx-5/6 enhancer. In order to test this hypothesis we used the C17 and MN9D neural cell lines (Choi et al. 1992; Snyder et al. 1992) and the different reporters listed in Figure 3i to assay for the effect of *Evf-2* on the activity of different enhancers. Figure 3a shows that *Evf-2* can increase the activity of reporters containing the conserved mouse Dlx-5/6 intergenic enhancers (mDlx ei + eii) or zebrafish Dlx-4/6 enhancers (zDlx ei + eii) in a dose-dependent manner. *Evf*-2-mediated activation is Dlx-2-dependent. In the C17 neural cell line, Dlx-2-mediated activation of the Dlx-5/6 enhancer is minimal, indicating that *Evf*-2 and Dlx-2 cooperate to increase activity of the enhancer.

We next asked whether the *Evf-2*/Dlx-2 cooperation acts through ei or eii, or requires the presence of both ei and eii targets. Figure 3b shows that ei and eii are independent targets of *Evf-2*/Dlx-2 cooperative activation, with greater activation through ei than eii. In addition, the activity of both ei + eii is not greater than ei alone, indicating a lack of synergy between ei and eii. The ability of *Evf-2* to activate either ei or eii suggests that an RNA:DNA base-pairing mechanism is unlikely to be involved in *Evf-2*/Dlx-2 cooperativity. Figure 3a also shows that both zebrafish and mouse ei + eii enhancers are targets of activation, consistent with their conserved activities in vivo (Zerucha et al. 2000).

Evf-2/*Dlx-2 cooperativity is both target and homeodomain specific*

A series of experiments to determine the specificity of the Dlx-5/6 DNA target and cooperation with Dlx-2 are described in Figure 3c–g. It has been shown previously that Dlx-2 activates the Wnt-1 enhancer (Iler et al. 1995) in the mouse C2C12 muscle cell line (Zhang et al. 1997). Figure 3c shows that *Evf-2* does not cooperate with Dlx-2 to increase the activity of the Wnt-1 enhancer, supporting the hypothesis that Evf-2/Dlx-2 cooperativity is Dlx-5/6 ei or eii target specific. Further support for target specificity is shown in Figure 3c where *Evf-2*/Dlx-2 does not increase the activity of the floor plate enhancer (Sasaki et al. 1997). In addition, *Evf-2* fails to cooperate with the zinc finger transcription factor Gli-1 (Kinzler et al. 1988), to activate the floor plate enhancer (Fig. 3c). Both the Wnt-1 and floor plate enhancers are below saturation levels, as reported previously (Zhang et al. 1997; Tyurina et al. 2005). Figure 3d shows that *Evf-2* does not cooperate with the paired homeodomain protein, Pax-3 (for review, see Mansouri 1998), or Gli-1 to activate the Dlx-5/6 enhancer. *Evf*-2/Dlx-2 cooperativity is observed in the MN9D (Choi et al. 1992) neural cell line (Fig. 3e), but not in the nonneural cell line, 293 (data not shown), suggesting that cell-type specific factors are required for cooperative activation. Since Msx genes are closely related to Dlx-2 and known to directly interact with Dlx-2 (Zhang et al. 1997), we tested whether *Evf-2* cooperates with Msx-1 or Msx-2 to repress the MyoD enhancer (Woloshin et al. 1995). Figure 3f shows that *Evf-2* fails to cooperate with Msx-1 or Msx-2, further supporting the specificity of the Dlx-2/*Evf-2* cooperativity.

We next asked whether other Dlx/*dll* homeodomain family members cooperate with *Evf-2* during Dlx-5/6 enhancer activation. Protein alignment of zebrafish Dlx family members (1, 2, 4, and 6) indicates that the homeodomain sequences are highly conserved between Dlx family members with only single amino acid differences in this region (data not shown). Figure 3g shows that the activity of different zebrafish Dlx family members listed from the most active to least is Dlx-2 > Dlx-4 > Dlx-6 > Dlx-1. Given that Dlx-4 is most similar to Dlx-2 and Dlx-1 is the least similar, these data suggest that the level of *Evf*-2/Dlx cooperative activity depends on relatedness to mouse Dlx-2. The difference between Dlx members is not a result of differential expression as verified by Western analysis (Fig. 3g). In a nonneural cell type, it was shown previously that Dlx-2 activates Dlx-5/6 enhancer activity in the absence of exogenous *Evf-2*. In this context, differences amongst Dlx/*dll* members were not detected (Zerucha et al. 2000). Taken together, these data suggest that the effects of *Evf*-2 on Dlx activity may occur in a subset of Dlx functions, rather than affecting all aspects of Dlx/*dll* signaling, and may depend on the presence of additional factors.

We next performed a series of experiments in order to understand the mechanism of the *Evf*-2/Dlx cooperation. It has been shown previously that Msx-1 and Msx-2 directly bind to Dlx-2 and inhibit activation of the Wnt-1 enhancer (Zhang et al. 1997). Thus one possible explanation for *Evf-2* transcription-enhancing activity is that *Evf-2* stabilizes Dlx-2 by preventing the inhibitory actions or binding of Msx. Figure 3h shows that Msx-1 and Msx-2 significantly inhibit *Evf-2*/Dlx-mediated cooperative activation of the Dlx-5/6 enhancer. Although these results do not rule out that *Evf-2* increases Dlx-2 activity by binding to inhibitory factors, it is clear that *Evf-2* does not prevent the repressor activity of the known inhibitors Msx-1 and Msx-2.

The active form of Evf-2 *is single-stranded RNA*

We next tested the efficiency of *Evf-2*/*Dlx-2* cooperation mediated by sense, antisense, and double-stranded *Evf-2* RNA. Figure 4a shows that sense *Evf-2* (I), but not antisense *Evf-2* (II), is the active form, and that the antisense form inhibits sense activity. In addition, double-stranded

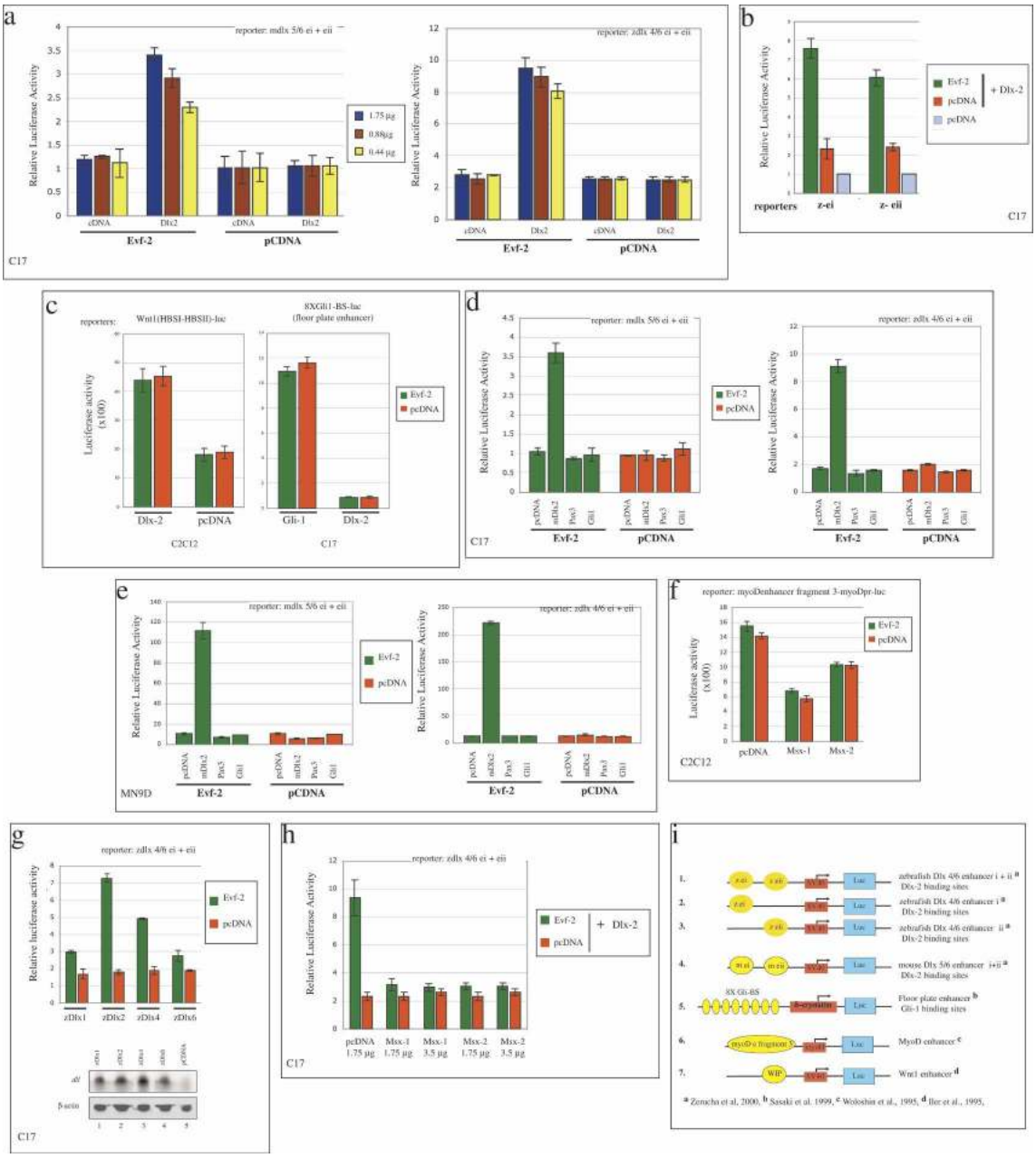

Figure 3. *Evf-2* cooperates with Dlx family members to activate Dlx-5/6 enhancer activity in a target-specific, homeodomain-specific, and cell-type-specific manner. The C17 and MN9D neural cell lines or the C2C12 muscle cell line, as indicated, were transfected with pcDNA-containing constructs along with the different reporters, as indicated (see *i*). All experiments were performed a minimum of three times in triplicate. The different reporters listed in *i* 1–7 were used as targets to determine the specificity required for cooperative activation by *Evf-2* and Dlx-2. Transfection efficiency was normalized by including a *Renilla luciferase* internal control plasmid. (*a*) Evf-2 induces dosage-dependent cooperative activation of the mouse Dlx-5/6 and zebrafish Dlx-4/6 enhancer constructs. Evf-2 (1.75, 0.88, or 0.44 µg) was cotransfected with pcDNA–Dlx-2, along with different reporter constructs, and *Firefly* and *Renilla luciferase* activities were determined, normalized, and plotted on the *Y*-axis. (*b*) Both ei and eii are targets of Evf-2 transcription-enhancing activity. (*c*) *Evf-2* does not cooperate with Dlx-2 to increase the activation of the Wnt enhancer and does not cooperate with Gli-1 to increase the activation of the floor plate enhancer. (*d*) *Evf-2* does not cooperate with Pax3 or Gli-1 to activate Dlx-5/6 enhancer activity in C17 neural cells. (*e*) *Evf-2* cooperates with Dlx-2 but not with Pax-3 or Gli-1 to activate Dlx-5/6 enhancer activity in MN9D neural cells. (*f*) *Evf-2* does not cooperate with Msx-1 and Msx-2 to suppress the myoD enhancer in the muscle cell line C2C12. (*g*) Dlx family members 1, 2, 4, and 6 exhibit cooperative activity with *Evf-2* to different levels, Dlx-2 > Dlx-4 > Dlx-6 > Dlx-1. Western analysis of transfected cell extracts probed with pan-anti-*dll* antibody is shown *below*. (*h*) *Evf-2* does not prevent inhibition by Msx-1 and Msx-2. (*i*) Summary of reporters used in *a*–*h*.

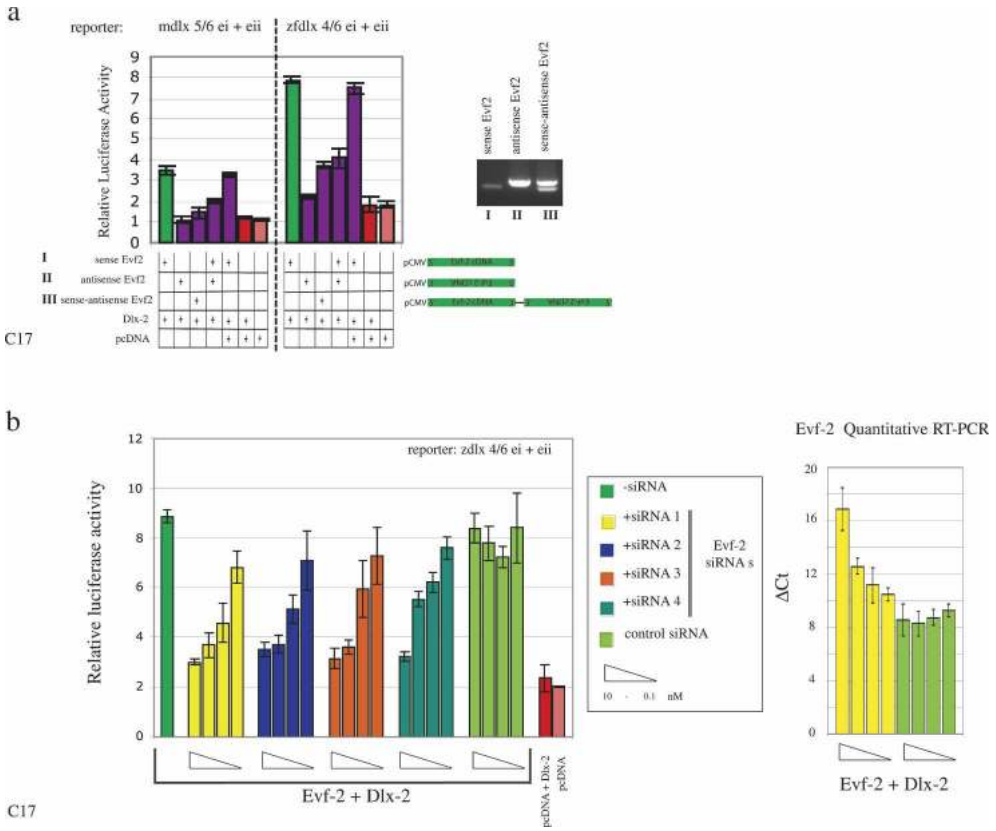

Figure 4. The active form of *Evf-2* is single-stranded RNA. (*a*) The sense (I), but not antisense (II) or double-stranded (III) form of *Evf-2* cooperates with Dlx-2 to increase the transcriptional activity of the Dlx-5/6 enhancer. Antisense decreases the activity of the sense form. RT–PCR of C17 cells transfected with constructs I, II, and III show that all three forms are made. (*b*) siRNAs (1–4) directed against *Evf-2* inhibit *Evf-2*/Dlx-2 transcriptional activation in a dose-dependent manner. siRNA-1 (yellow bars) degrades *Evf-2* RNA levels as assessed by quantitative RT–PCR, whereas a control siRNA generated against luciferase (green bars) does not. (ΔCt) Number of Evf-2 cycles minus the number of β-actin cycles, repeated three times and averaged.

Evf-2 made on a colinear strand (Fig. 4a, sense–antisense, III) is threefold less active than sense alone. RT–PCR analysis verifies that forms I, II, and III are made in transfected cells. In addition, we can also detect III with a primer set that spans the sense–antisense junction (data not shown). We next asked whether siRNAs directed against *Evf-2* are able to inhibit *Evf-2* transcription-enhancing activity. Figure 4b shows that four different siRNAs against *Evf-2* inhibit transcriptional activation in a dose-dependent manner. As shown by quantitative RT–PCR, at its highest concentration (10 nM) siRNA 1 (Fig. 4b, yellow bars) increases the number of cycles necessary to detect *Evf-2* RNA from eight (Fig. 4b, control siRNA, green bars) to 17 cycles (Fig. 4b). This nearly complete degradation of *Evf-2* by siRNA 1 at its highest concentration eliminates the effects of *Evf-2* on transcriptional activity. These data provide support that the effects of *Evf-2* on transcription are mediated at the RNA, and not DNA level. Taken together, these data suggest that the *Evf-2* transcription-enhancing activity requires single-stranded sense RNA, and the following constraints on specificity: Dlx-5/6 target DNA, Dlx homeodomain protein, and cell-type.

The Evf-2 *5′ region is both necessary and sufficient for activity*

In order to define the *Evf-2* active regions, a series of deletions were tested for cooperative activity (Fig. 5). Deletion analysis shows that the 5′ region is critical for activity, with a significant reduction in *Evf-2* activity when nucleotides 117–563 are deleted. In addition, a fragment containing the *Evf-2* ei region between nucleotides 1–395 retains 85% of full-length *Evf-2* activity. In the absence of information regarding other transcriptionally active ncRNAs, and the absence of homology with ncRNAs, further definition of this region will be necessary to determine the precise nucleotides that are involved in *Evf-2*/Dlx-2 cooperativity and the role of secondary structure in this interaction.

Although ORFs >200 bp were not found within *Evf-2*, definition of the minimal transcription-enhancing region allowed further examination of the possibility that small peptides may be functioning instead of the RNA. The Evf-2 minimal transcription-enhancing region contains one possible conserved 19-amino-acid peptide. Although our data has not ruled out the possibility that

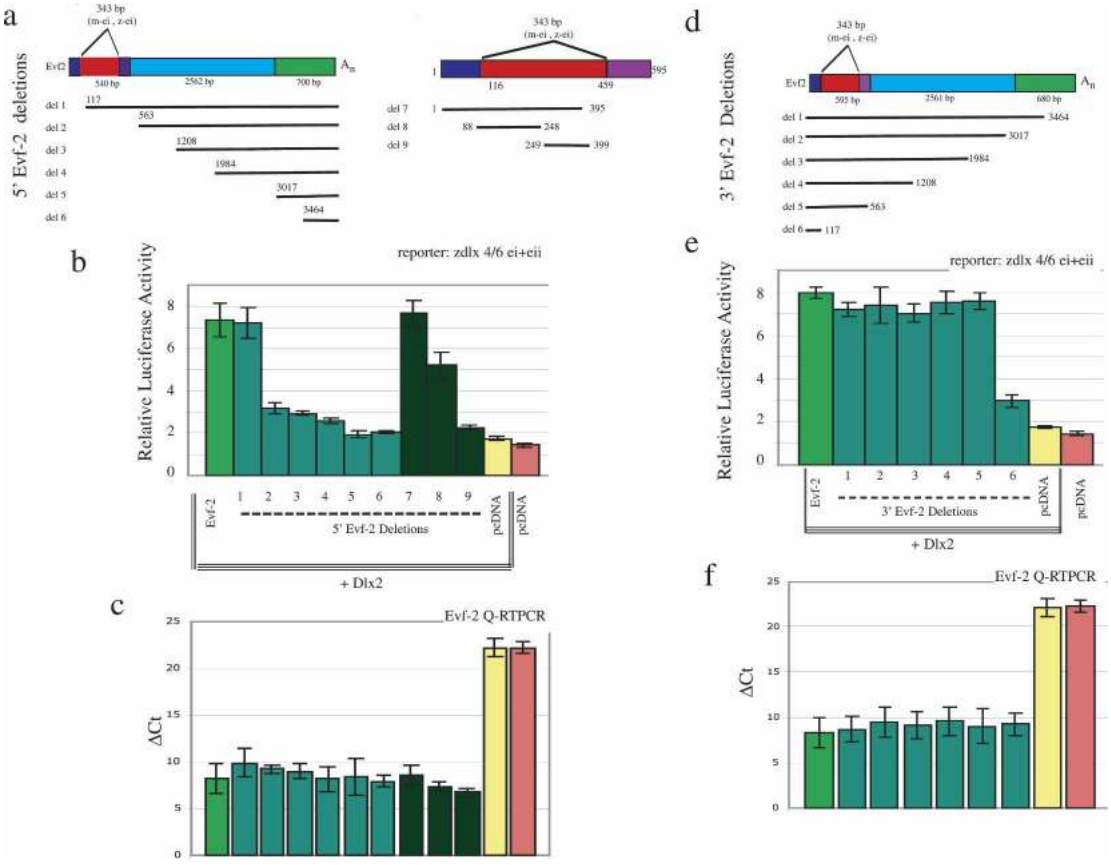

Figure 5. The *Evf-2* 5′ region is both necessary and sufficient for Dlx-2-dependent cooperative activation of the Dlx-5/6 enhancer. Comparison of Dlx-5/6 enhancer activation in C17 neural cell lines by different *Evf-2* deletion mutants. (*a*) Diagram of 5′ *Evf-2* deletions. (*b*) Activity of different 5′ Evf-2 deletions. (*c*) Quantitative RT–PCR of Evf-2 deletions. (*d*) Diagram of 3′ *Evf-2* deletions. (*e*) Activity of different 3′ Evf-2 deletions. (*f*) Quantitative RT–PCR of 3′ *Evf-2* deletions. Quantitative RT–PCR analysis shows that 5′ and 3′ deletions are made in relatively similar amounts. Therefore, loss of function is not the result of *Evf-2* RNA degradation. (ΔCt) Number of Evf-2 cycles minus the number of β-actin cycles, repeated three times and averaged.

this peptide is made, the lack of a nuclear localization signal together with the colocalization of the *Evf-2* RNA/Dlx-2 complexes in vivo (see below) suggest that this putative peptide is unlikely to play a direct role in transcriptional regulation.

Evf-2 and Dlx-2 form a complex in vivo

The interaction of transcription factors, in particular the *bicoid* homeodomain protein with both DNA and RNA has been reported previously (Dubnau and Struhl 1996; Cassiday and Maher 2002), raising the possibility of a direct interaction between the Dlx-2 protein and the *Evf-2* ncRNA. Support that the *Evf-2* ncRNA may directly affect Dlx-2 activity is shown in Figure 6a where *Evf-2* ncRNA/Dlx-2 complexes are detected in C17 cells cotransfected with a Flag-tagged Dlx-2 and a pcDNA–Evf-2 construct. Complexes between Flag-tagged Emx-1 (Simeone et al. 1992) and *Evf-2* are not detected, verifying the specificity of the *Evf-2*/Dlx-2 complex. We next asked whether *Evf-2*/Dlx-2 complexes form in the embryo in vivo. Complexes of *Evf-2*/Dlx are detected in E11.5 rat embryonic BA nuclear extracts by immunoprecipitation with anti-*dll* antibody and subsequent RT–PCR for *Evf-2* (Fig. 6b). BAs were chosen because they have been shown previously to contain high levels of *Evf-1* (Kohtz and Fishell 2004). In order to rule out that *Evf-2*/Dlx complexes arise during the process of making nuclear extracts, we next wanted to determine if *Evf-2*/Dlx complexes can be visualized in single cells. Figure 6c shows that in vivo complexes of *Evf*-2 RNA and Dlx proteins can be visualized in single cells made from E12.5 ventral telencephalon by fluorescent in situ hybridization and coimmunolocalization using anti-*dll* antibody. Zeiss 510 Meta confocal analysis shows two bright spots in the nucleus bound by *Evf-2* antisense RNA probes (Fig. 6c, red) colocalizing with anti-*dll* (Fig. 6c, green) to generate bright-yellow spots. DAPI (Fig. 6c, blue) colocalization shows that staining is in the nucleus. *Evf-2*/Dlx staining was not observed in cells made from tissue that does not express *Evf-2* or Dlx (E12.5 dorsal telencephalon) (Fig. 6c) or with other antisense RNA probes tested (Dlx-5, Emx-1, or in the absence of *Evf-2* antisense RNA probe) (data not shown). The fluorescent pattern of two bright intranuclear *Evf-2* spots is consistent with that found in tissue sections

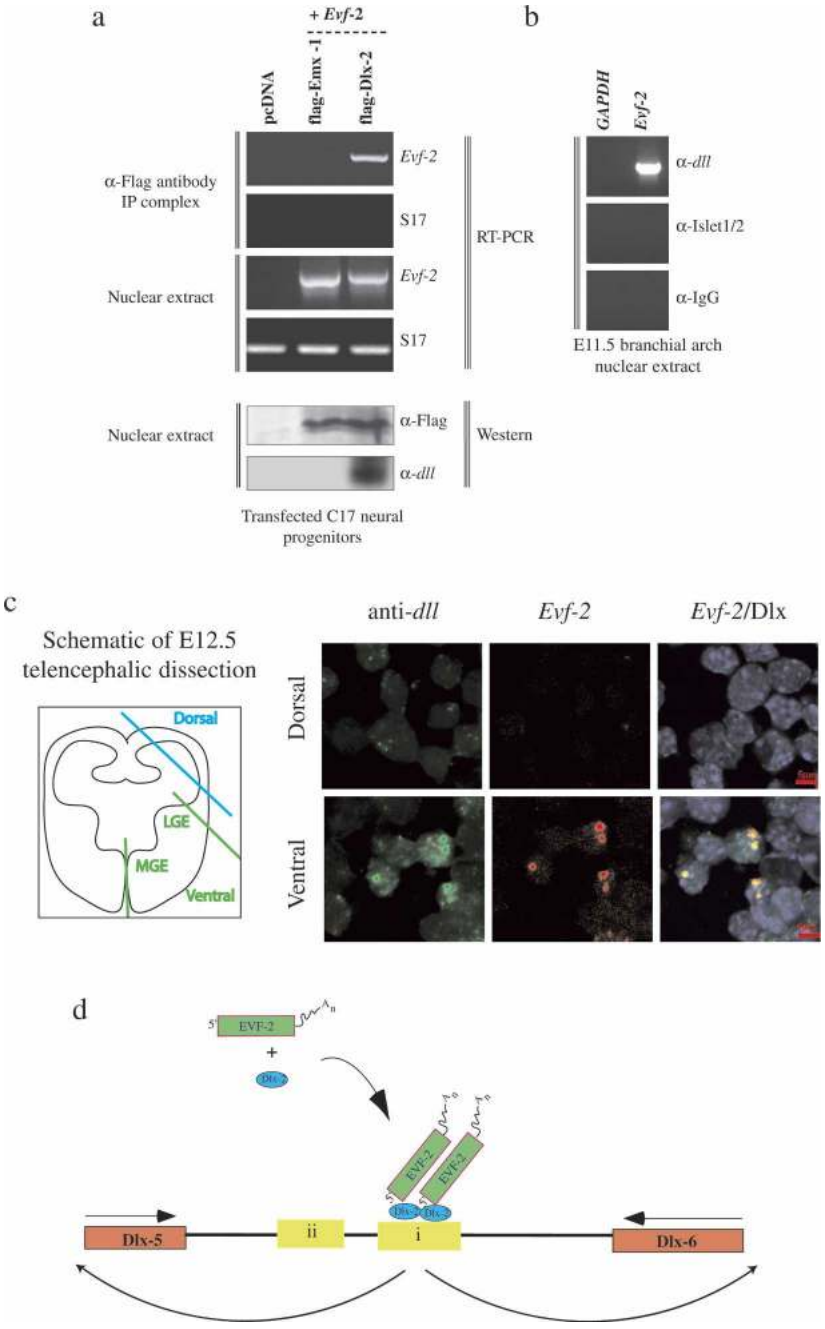

Figure 6. *Evf-2* and Dlx-2 form a complex in vivo. (*a*) Nuclear extracts made from C17 neural cells transfected with Flag-tagged Emx-1, Flag-tagged Dlx-2, or pcDNA control were analyzed for the presence of *Evf-2*–Dlx-2 complexes by immunoprecipitation with anti-Flag antibody, followed by RT–PCR against *Evf-2*-specific primers and S17 control primers. Western analysis shows that both Flag-Emx-1 and Flag-Dlx-2 are present in nuclear extracts transfected with constructs expressing these proteins. (*b*) Nuclear extracts made from rat E11.5 BAs were analyzed for the presence of *Evf-2*/Dlx-2 complexes by immunoprecipitation with anti-*dll*, anti-Islet 1/2, or anti-IgG antibody, followed by RT–PCR against *Evf-2*-specific primers or GAPDH. (*c*) Single-cell suspensions made from mouse E12.5 dorsal and ventral telencephalon were dissected as shown in the schematic, centrifuged onto slides, and processed for fluorescent in situ/immunolocalization using *Evf-2* antisense RNA probe and anti-*dll* antibody. DAPI staining (blue) reveals nuclei. *Evf-2* RNA (Alexa fluor 568) is in red, Dlx (Alexa fluor 488) is in green, and regions of overlap are in yellow. (*d*) A model proposing that a complex of *Evf-2* and Dlx-2 affects ei activity, ultimately affecting transcription of the Dlx-5 and Dlx-6 genes.

vivo (see Fig. 1f, panel ii). These data show that *Evf-2* RNA and Dlx proteins form stable in vivo complexes. It was demonstrated previously that Dlx-2 binds ei DNA sequences in a gel shift assay (Zerucha et al. 2000) as well as CHIP analysis (Zhou et al. 2004). Together, these data suggest that the *Evf-2*/Dlx-2 complex stabilizes the interaction between Dlx-2 and target Dlx-5/6 enhancer sequences to increase transcriptional activity. A model of one possible mechanism is shown in Figure 6d. In this model, *Evf-2* binds to Dlx-2 in a DNA-independent manner, and the entire complex binds to the enhancer site. Although not shown in the model, the intensity of the Dlx signal in the spots suggests that multiple copies of *Evf-2*/Dlx-2 complexes are being visualized. These complexes may be associated with Dlx-2 bound to DNA as shown in the model, or only serve to stabilize Dlx-2 before it binds to the DNA. Future experiments to distinguish between these possibilities and to determine the nature of the *Evf-2*/Dlx-2/DNA interaction will be critical for understanding the exact mechanism of this type of transcriptional regulation.

Discussion

The Dlx genes—individually and in combination—are critical for the differentiation and migration of neurons

in the brain. How this important family of genes is regulated is poorly understood. In this report we show that the *Evf*-2 ncRNA, partially encoded by the Dlx-5/6 ultraconserved region, complexes with the Dlx-2 protein and enhances Dlx-2 activity in a target and homeodomain-specific manner. We propose that *Evf-2* belongs to a new class of trucRNAs that have evolved to regulate genes critical for generating diversity in vertebrates—in particular the brain, the most complex organ in the animal kingdom.

Similarities with known noncoding RNAs

Similarities between *Evf*-2 and the previously characterized ncRNAs H19 (for review, see Arney 2003), Air (Sleutels et al. 2002), *roX* (Amrein and Axel 1997; Meller et al. 1997), and SRA (Lanz et al. 1999) are apparent. H19 and *Evf-2* were isolated in a differential expression screen, are developmentally regulated, polyadenylated, and spliced. Their sizes are similar (H19 = 2.3 kb, *Evf-2* = 3.8 kb). Both H19 and the transcription-enhancing region of *Evf-2* contain no ORFs >200 bp by cross-species sequence conservation analysis and testing by in vitro translation. While it has been shown that the H19 ncRNA does not play a role in imprinting the Igf2 locus, a DNA element located near the H19 promoter (H19-DHR) has been found to influence the imprinting of the Igf2 locus (Schmidt et al. 1999; Hark et al. 2000). The *trans*-acting effects of the H19 ncRNA have been linked to tumor suppression, but a mechanism has not been identified. The relationship of Air (a 108-kb polyadenylated, nonspliced ncRNA) transcription to an imprinting control element (ICE) and antisense transcription to the Igf2r promoter (Wutz et al. 2001; Zwart et al. 2001) may be similar to the relationship between Evf-2, the Dlx-5/6 enhancer, and the Dlx-6 promoter. The promoter of the Air ncRNA overlaps with the ICE element and premature transcription termination of Air results in silencing of three genes in the region, two of them nonoverlapping with Air (Sleutels et al. 2002). The ability of the *roX* RNAs to activate transcription of the X chromosome in *Drosophila*, as well as roX DNA to serve as a chromosome entry point for activation may be mechanistically similar to *Evf-2*. While DNA target specificity of *trans*-acting *roX* ncRNAs has not been found, a short 217-bp roX1 DNA fragment is sufficient to produce an ectopic chromatin entry site (Kageyama et al. 2001). Recruitment by roX1 DNA was *roX1* ncRNA independent (Kageyama et al. 2001). Given the results obtained with roX1 DNA and RNAs, it will be important to determine whether the *Evf-2*/Dlx-2 complex on the Dlx-5/6 enhancer functions similarly as a specific chromosome entry point. Finally, the specificity and coactivator function of *Evf*-2 is similar to SRA, an ncRNA that specifically coactivates steroid hormone receptor activity (Lanz et al. 1999). However, since that report, additional examples of ncRNAs acting as specific transcriptional coactivators have not appeared. Given both the significant similarities and differences between *Evf-2* and existing ncRNAs, we propose that *Evf-2* belongs to a novel class of transcription-regulating ncRNAs (trRNAs) that specifically influence the activity of homeodomain-containing transcription proteins.

Dual roles for RNA and DNA in homeodomain transcriptional regulation

Similar to the increased acceptance of new roles for RNAs in biological processes is the idea that dual functions can be attributed to a single molecule. This idea is not only relevant when looking at the *H19*, *Air*, *roX*, and *Evf-2* examples, where a gene sequence may function at both the level of DNA and RNA, but also in the action of transcription factors. Recent reports of transcription factors that bind DNA and RNA with distinct roles have been reported (for review, see Cassiday and Maher 2002). Three demonstrated (and more hypothesized) examples of this include the following: TFIIIA, a zinc finger-containing transcription factor that binds both 5S rDNA and 5S rRNA (Engelke et al. 1980; Clemens et al. 1993), tra-1, another zinc finger transcription factor that regulates developmental genes and binds the tra-2 mRNA 3′ untranslated region (UTR) (Graves et al. 1999), and bicoid, a homeodomain-containing transcription factor that regulates developmental genes and suppresses cad mRNA translation by binding to the cad mRNA 3′UTR (Dubnau and Struhl 1996). In our studies, we show that Dlx-2, a homeodomain-containing transcription factor, known to bind and activate the Dlx-5/6 enhancer, cooperates with the *Evf-2* ncRNA resulting in an increase of Dlx-5/6 enhancer activity. Whether Dlx-2, like bicoid, binds both DNA and RNA during the cooperative interaction, or whether *Evf-2* sequesters a transcriptional inhibitor independent of binding to Dlx-2 directly, remains to be determined. However, the presence of *Evf-2*/Dlx-2 complexes in two concentrated spots within the nucleus supports a direct role of the *Evf-2* ncRNA on Dlx-2 transcriptional activity. Although the model in Figure 6d proposes that *Evf-2* ncRNAs remain associated with Dlx-2 after Dlx-2 binds to its target, an alternative possibility is that *Evf-2*/Dlx-2 complexes do not form directly on the DNA target site. Instead, *Evf-2*/Dlx-2 complexes may be a reservoir for active Dlx-2 protein. Further characterization of the *Evf-2*/Dlx-2 complex will need to be performed in order to distinguish between these possibilities.

Target-specific transcriptional regulation, a common mechanism for homeodomain transcriptional regulation?

Reports that the 7SK snRNA (Nguyen et al. 2001; Yang et al. 2001) and 6S RNA (Wassarman and Storz 2000) affect transcription by modulating RNA polymerase activity and more recently, the repression of RNApolIII-dependent transcription by the pole cell granule (*pgc*) ncRNA in *Drosophila* germ cells (Martinho et al. 2004), show that RNAs can effect transcription through a general mechanism. Our work shows that, unlike the 7SK

snRNA and 6S RNA, and possibly *pgc* ncRNA, *Evf*-2 is a developmentally regulated ncRNA that affects transcriptional activity by cooperation and complex formation with a developmentally regulated homeodomain protein rather than by affecting the general transcriptional machinery through interactions with an RNA polymerase. This raises the possibility that other conserved nonprotein coding regions and enhancer sequences may be transcribed to generate polyadenylated ncRNAs capable of self-activation and transcription factor complex formation. If undiscovered families of ncRNAs that regulate the activity of different enhancer targets exist, why are there no previous reports of these regulators? One possibility is that ncRNAs isolated on the basis of restricted expression may have been discarded as noncoding and therefore nonfunctional. Another possibility is that, although single mutations may cause frame shifts and truncations in proteins coded by mRNAs, single mutations are less likely to affect ncRNA function. Our decision to test the *trans*-acting effects of *Evf-2* on enhancer activity was based on the identity of the 5′ region of *Evf-2* with the evolutionarily and functionally conserved Dlx-5/6 enhancer ei sequences. Given that conserved intergenic regions have been identified for other Dlx loci (Ghanem et al. 2003), that 97% of the human genome is noncoding with numerous putative and demonstrated noncoding transcripts, and that comparisons between the human and Fugu genomes reveal multiple conserved noncoding sequences (Gilligan et al. 2002), our results suggest that it will be important to consider the role of enhancer and conserved nonprotein coding sequences in transcriptional regulation at both the DNA and RNA levels.

Ultraconserved regions, Shh signaling, and neuronal diversity

Key experiments in the spinal cord suggest that the establishment of a gradient of Shh signaling produces combinatorial homeodomain expression patterns, which in turn give rise to diverse neurons (Briscoe and Ericson 2001). However, it is presently not known whether neuronal diversity and/or function also depend on the relative level of expression of each homeodomain protein. In this report, we show that Shh activation results in the coexpression of *Dlx-2*, *5*, and *6* and *Evf-2* transcripts in the brain. Recent data suggest that MECP2-null mice exhibit as little as a twofold up-regulation in Dlx-5 expression and that a loss of Dlx-5 imprinting is observed in Rett syndrome patients (Horike et al. 2005). That such small changes in Dlx-5 expression may alter neuronal function raises the possibility that the levels of homeodomain protein expression within neurons may also be critical for generating different types of neurons and/or determining neuronal function. Even more recently, it was shown that the loss of Dlx-1 results in the loss of specific neuronal subtypes in the brain (Cobos et al. 2005). Taken together, these data raise the possibility that the Shh ventralizing signal in the brain activates Dlx homeodomain proteins responsible for generating diversity as well as trRNAs such as *Evf-2* for subtle regulation of these genes, providing an additional mechanism to generate neuronal diversity in the brain.

One of the surprising outcomes of large-scale genomic comparisons between human and fish is the number of ultraconserved DNA regions (UCRs) located close to genes coding for transcription factors involved in developmental control, including several homeodomain proteins in the Shh pathway (Sandelin et al. 2004; Woolfe et al. 2005). These screens suggest that UCRs acting as transcriptional control elements with 90% or greater conservation are scattered throughout the vertebrate, but not invertebrate, genome. The average length of these regions (500 bp) is too long to explain their function solely as DNA-binding targets. However, this length is consistent with the hypothesis that trRNAs such as *Evf-2* (trucRNAs) may be transcribed from a subset of UCRs, thereby controlling the expression of adjacent transcription factors at two levels. Support for a conserved functional role of *Evf-2* in vertebrates stems from our finding that the conservation of *Evf-2* in vertebrates (humans, rodents, zebrafish, and chicken) is limited to the region identified as the transcription-enhancing functional region (Figs. 1a [green bar], 5). If other UCRs are transcribed to generate trRNAs, this would raise the possibility that trucRNAs have evolved to modulate levels of homeodomain proteins within particular neurons in order to increase neuronal diversity and the complexity that was required during the expansion of the vertebrate nervous system, particularly in the brain.

Materials and methods

Isolation of Evf-1 *and* Evf-2

Differential display, isolation of *Evf-1*, and in situ hybridization were described previously (Kohtz and Fishell 2004). The 3836-bp Evf-2 cDNA was isolated from a rat embryonic brain E15.5 library (Jim Boulter, Salk Institute, La Jolla, CA) using the Evf-1 cDNA as a probe (Kohtz and Fishell 2004). Reporter assays were performed using the C17 neural cell line (Snyder et al. 1992) between passages 5 and 7, MN9D (Choi et al. 1992), or C2C12 (ATCC). Luciferase assays were performed using a dual-luciferase assay kit (Promega) using lipofectamine (Invitrogen). All transfections were normalized with an internal control expressing *Renilla luciferase*, performed in triplicate and a minimum of three times. At C17 passages >7 (8–12) *Evf-2*/Dlx-2 cooperative enhancer activation was not detected (data not shown). In order to verify that *Evf-2* functions as a single-stranded RNA, the following primers were used in Figure 4a:

Specific primers for reverse transcription: Rat Evf-2 sense, 5′-AGAGAGATTCTCTGGGGTCC-3′ and Rat Evf-2 antisense, 5′-AGGCATGCTACCTACAGGAT-3′.

PCR primers: Rat Evf-2 sense-forward, 5′-AGAGAGATTCT CTGGGGTCC-3′; Rat Evf-2 sense-reverse, 5′-TCAGTCAGTC TTCAGAATGG-3′; Rat Evf-2 antisense-forward, 5′-AGGCAT GCTACCTACAGGAT-3′; and Rat Evf-2 antisense-reverse, 5′-GGAGTCCAGATAAATGAGTG-3′.

cDNAs were obtained from zebrafish embryos and chick embryonic brains at 24 and 36 h post-fertilization, respectively.

PCR primers: Zebrafish ei-forward A, 5′-GGATCGATCCT GAACAAAGC-3′; Zebrafish ei-reverse A, 5′-GTTTCGTCTTT

GCCACTTCA-3′; Zebrafish ei-forward B, 5′-ATTTATGGGT TTTATCCAAGAGAGG-3′; Zebrafish ei-reverse B, 5′-CCACT TCAAATCCAAATAAAGATGC-3′; Zebrafish Dlx-2-forward, 5′-TCGTTGGACTTGCTTTTAAG-3′; Zebrafish Dlx-2-reverse, 5′-TTTCAGCATCTGCAGGAGTT-3; Chick ei-forward A, 5′-CCCCTTCCCACTGTGAAACT-3′; Chick ei-reverse A, 5′-CTTTCCTGTTCCCGAATCTA-3′; Chick ei-forward B, 5′-GAACAAAGCCTCCAGCTGCA-3′; Chick ei-reverse B, 5′-CCTTTCCTGTTCCCGAATCT-3′; Chick Dlx-2-forward, 5′-CTCCCACTTTACCCGAGTCC-3′; and Chick Dlx-2-reverse, 5′-CTTCTGGAACCTCCTCTGCA-3′

In Figure 4b, the control siRNA was supplied with the Silencer siRNA Construction Kit (Ambion, catalog no. 1620) and siRNAs directed against the following Evf-2 sequences were constructed using the same kit: siRNA 1, 5′-AATTTGTGTAT GAATAACAGA-3′; siRNA 2, 5′-AATTTCCCTCTTTTGTT TCGC-3′; siRNA 3, 5′-AAAGATGGCTTTTTAGTATTA-3′; and siRNA 4, 5′-AAGTGGAAGAAAATTACAGGT-3′.

Immunoprecipitation of Evf-2/*Dlx-2 complexes*

In order to detect complexes of *Evf-2* and Dlx-2, nuclear extracts (Dignam et al. 1983) were prepared from transfected C17 cells (1 × 150-cm plate, resuspended in a final volume of 500 µL) or E11.5 rat embryonic BA nuclear extracts (~72 embryos, resuspended in a final volume of 60 µL). Twenty microliters of BA nuclear extract or 25 µL of C17 nuclear extract was incubated with 125 µg of heparin and 10 µg of tRNA for 5 min at room temperature, then preabsorbed with protein G-agarose in 500 µL of PBS + 0.1% Triton X-100 + protease inhibitor cocktail (Sigma) (PBS-T) for 1 h at 4°C. The C17 nuclear extracts were then incubated with mouse anti-Flag (Sigma) prebound to protein G-agarose, whereas the BA nuclear extracts were incubated with anti-*dll (*affinity-purified as described by Panganiban et al. [1995]), anti-Islet 1/2 (40.2D6, Developmental Hybridoma Studies Bank), or anti-rabbit IgG prebound to protein G-agarose overnight at 4°C. The bound complexes were washed three times with PBS-T, resuspended in nuclease-free water, and treated with DNase I (NEB). RT–PCR was performed on bound complexes using MMoLV RT (Invitrogen), random primers (New England Biolabs), and Taq DNA polymerase (Invitrogen). The PCR primers were as follows:

C17 complex: Evf-2, forward primer, 5′-AATTGGATGGCAC TGCAGC-3′; Evf-2 reverse primer, 5′-AAGACTGGACAGC CATCACG-3′; S17 forward primer, 5′-AAGCTCCGCAACAA GATAGC-3′; and S17 reverse primer, 5′-TGAAGGTTGGAC AGACTGCC-3′.

BA complex: Evf-2-forward primer, 5′-GATGTCTCCTGAA TGACTCTA-3′; Evf-2-reverse primer, 5′-TGCTTCAAGGTC AATGGCTGG-3′; r-GAPDH-forward primer, 5′-CCTTCATT GACCTCAACTAC-3′; and r-GAPDH-reverse primer, 5′-TCT TCTGAGTGGCAGTGATG-3′.

Rabbit anti-*dll* was made by injecting the *dll* 42-amino-acid homeodomain fragment (Panganiban et al. 1995) cross-linked to KLH, and affinity-purified on a column containing the *dll* 42-amino-acid homeodomain fragment by AKTA FPLC affinity chromatography (Amersham/Pharmacia). The antibody was verified for specificity by Western analysis (see Fig. 3g) and immunolocalization as shown previously (Kohtz et al. 2001; Feng et al. 2004).

Real-time PCR, primers, and probes

Real-time PCR was performed to quantitate the levels of Evf-2 RNAs in transfected C17 cells. Total RNA was prepared by using Trizol reagent (Invitrogen) and treated with RNase-free DNase I (NEB) prior to the assay. Specific primers (Integrated DNA Technologies) and TaqMan probes (MegaBases) were designed by Primer Express computer software (Perkin-Elmer/ABI). Real-time PCR was performed by ABI Prism 7700 Sequence Detector System (Perkin-Elmer/ABI) using the TaqMan PCR Core Reagent Kit (Applied Biosystems, Roche) according to the manufacturer's instructions. Thermal cycler conditions were as follows: 30 min at 48°C, then 15 min at 95°C, followed by 40 cycles of 15 sec at 95°C, 1 min at 59°C. Quantitation of the sample is based on the cycle when the amplicon is first detected, threshold cycle (Ct) as defined by Higuchi et al. (1993). Results were normalized according to levels of β-actin, with ΔCt = Ct(Evf-2) – Ct(β-actin).

Primers and probes for quantification of Evf-2 and Evf-2 deletions

Evf-2 5′ deletions 1–6: r-Evf2 3′end-forward, 5′-ACCCATAGA ATTCCAACCGTTCT-3′; r-evf2 3′end-reverse, 5′-AGATGCT CGGAGCTTTCACACT-3′; and r-evf2 3′end Taqman probe, 5′-AACGTTCTGCTGAGCACCTCACACTTC-3′.

Evf-2 3′ deletions 1–6, Evf-2 5′ deletion 7, and Evf-2 targeted by siRNA degradation: r-Evf2 5′end-forward, 5′-CGGCACG AGGACAGAGCT-3′; r-evf2 5′end-reverse, 5′-AAGCAATGAT CAGGGTCTAGAAATCT-3′; and r-evf2 5′end Taqman probe, 5′-ATACTCTCCTGTGCCTCGGCTC-3′.

Evf-2 deletions 8 and 9: r -Evf2 del 8-forward, 5′-CATTG CTTAAGAGAGATTCTCTGGG-3′; r-Evf2 del 8-reverse, 5′-TCAGGAACAGGAAAGGCGAA-3′; r-evf2 del 8 TaqMan probe, 5′-TCCTCAGTCTCTGCAATTTGTGTATGAATAA CA-3′; r-Evf2 del 9-forward, 5′-CGCTGTAATCAGCGGGCTA CATGA-3′; r-Evf2 del 9-reverse, 5′-TGCAGTGCCATCCAAT TTGA-3′; and r-Evf2 del 9 TaqMan probe, 5′-AATTACTCT AATTATGGCTGCATTTAAGAGAATGGAA-3′.

Mouse β-actin: m-β-actin-F, 5′-ACGGCCAGGTCATCAC TATTG-3′; m-β-actin-R, 5′-CAAGAAGGAAGGCTGGAAAA GA-3′; and m-β-actin TaqMan probe, 5′-CAACGAGCGGTTC CGATGCCCT-3′.

RNA in situ hybridization

The mouse Dlx-6 in situ probe was obtained by RT–PCR from E12.5 mouse brain (forward primer, 5′-GGGGACGACACAG ATCAACA-3′ and reverse primer, 5′-TACCCCGGCATGTAG CTGTT-3′; Tm = 55°C), cloned into pGEM-T Easy Vector System I (Promega), linearized with SalI, and transcribed with Sp6 polymerase using a Digoxigenin labeling kit (Roche). Dlx-5 and Dlx-2 were obtained from John Rubenstein (University of California at San Fancisco, San Franciso, CA), and Shh was obtained from Doug Epstein (University of Pennsylvania, Philadelphia, PA). Section in situ hybridizations were performed according to Schaeren-Weimers and Gerfin-Moser (1993), except embryos were fixed in 4% paraformaldehyde overnight at 4°C and incubated in 30% sucrose before embedding in Tissue Tek Optiomal Cutting Temperature (OCT). In addition, slides were treated with a permeabilization step (PBS + 1%Triton X-100 for 1 h at room temperature) prior to prehybridization.

Evf-2 *RNA in situ/Dlx immunolocalization*

Dissections of embryonic mouse brains were performed using Lumsden Bioscissors (Dr. Andrew Lumsden, King's College, London, UK) in ice-cold L-15 medium (Gibco). Approximately 200 µL of prewarmed 0.1% trypsin was added to dissected tissue from 10 embryos for 15 min at 37°C, and trypsin-inactivated with 10 µL of goat serum. Cell clumps were dispersed by pipet-

ting gently and were centrifuged at 1500 rpm for 5 min at 4°C. The pellet was resuspended in 500 µL of L-15 media. Cells (5×10^5) in a volume of 500 µL were centrifuged onto slides at 1000 rpm for 4 min (Shandon Cytospin). Cells were fixed in 4% paraformaldehyde for 10 min at room temperature, rinsed in PBS, and processed for in situ hybridization. Slides were digested with proteinase K (1 µg/mL) in 50 mm Tris + 5 mm EDTA for 5 min at room temperature, refixed in 4% paraformaldehyde in PBS fo 5 min at room temperature, and washed three times in PBS at room temperature. Slides were then incubated in acetylation buffer (300 mL H_2O + 5.5 g of triethanolamine + 672 µL of 10 N NaOH) to which 750 µL of acetic anhydride was added drop-wise for 10 min at room temperature, washed three times in PBS at room temperature, and incubated in 1% Triton-X in PBS for 1 h at room temperature. Slides were quenched for endogenous peroxidase in 1% hydrogen peroxide in PBS for 30 min at room temperature, and washed three times in PBS. Three-hundred microliters of prehybridization buffer was added on each slide and parafilm cover-slipped overnight at room temperature. Hybridization using digoxigenin-labeled antisense Evf-2 probe was performed overnight at 72°C, and slides were rinsed in 5× SSC, washed in 0.2× SSC for 1 h at 72°C, and rinsed in 1× PBS at room temperature. The slides were then processed for tyramide labeling according to the manufacturer's instructions (Molecular Probes), using the anti-mouse IgG, tyramide-Alexa fluor 568 kit first. Slides were incubated overnight at 4°C with mouse anti-digoxigenin (0.1 µg/mL, Roche) and rabbit anti-*dll* (1:700). After incubation with the Alexa fluor 568, slides were quenched again with 1% hydrogen peroxide/PBS for 30 min at room temperature to inactivate any residual HRP activity, and washed three times in PBS before proceeding with visualization of anti-*dll* with the anti-rabbit IgG, tyramide-Alexa fluor 488 kit. The HRP conjugates and tyramides were both used at 1:100. Slides were incubated with DAPI for 5 min at room temperature before mounting in Fluorosave (Calbiochem). A Zeiss confocal 510 Meta with AIM software was used to visualize intranuclear fluorescence.

Acknowledgments

We thank the following investigators: Marc Ekker (Ottawa Institute), for sending the Dlx-5/6 and Dlx-4/6 ei and eii GFP plasmids for the initial work prior to publication, and for many helpful discussions; John Rubenstein (University of California at San Francisco) for the Dlx-2 and Dlx-5 cDNA probes for in situ; Nick Gaiano (Johns Hopkins University) for advice and training on mouse embryonic ultrasound-guided injections and viral production; Cory Abate-Shen (University of Medicine and Dentistry of New Jersey) for sending the Msx-1 cDNA, Msx-2 cDNA, Wnt-1–luciferase, and MyoD–luciferase reporter constructs; Doug Epstein (University of Pennslvania) for mouse Shh cDNA; Evan Snyder (Harvard University) for the early passage C17-2 neural cell line; Alfred Heller (University of Chicago) for the MN9D neural cell line; Grace Panganiban (University of Wisconsin) for the construct encoding the *dll* homeodomain; Hiroshi Sasaki (Osaka University) for the floor plate enhancer construct; Phil Iannoccone (Northwestern University) for Gli-1-pcDNA; and Jim Boulter (Salk Institute) for the rat embryonic brain E15.5 library. We also thank Jacek Topczewski (Northwestern University) for cDNAs from zebrafish embryos. This work was initially funded by a Howard Hughes Young Investigator Award (to J.D.K.), an Illinois Excellence in Academic Medicine Award (Children's Memorial Hospital, Chicago), and currently NIH/NICHD HD044745 and R21HD049875 (to J.D.K.).

References

Acampora, D., Merlo, G.R., Paleari, L., Zerega, B., Postiglione, M.P., Mantero, S., Bober, E., Barbieri, O., Simeone, A., and Levi, G. 1999. Craniofacial, vestibular and bone defects in mice lacking the *Distal-less* related gene *Dlx5*. *Development* **126:** 3795–3809.

Akhtar, A. 2003. Dosage compensation: An intertwined world of RNA and chromatin remodeling. *Curr. Opin. Genet. Dev.* **13:** 161–169.

Amrein, H. and Axel, R. 1997. Genes expressed in neurons of adult male *Drosophila*. *Cell* **88:** 459–469.

Anderson, S., Eisenstat, D., Shi, L., and Rubenstein, J. 1997a. Interneuron migration from basal forebrain to neocortex: Dependence on *Dlx* genes. *Science* **278:** 474–476.

Anderson, S.A., Qiu, M., Bulfone, A., Eisenstat, D.D., Meneses, J., Pedersen, R., and Rubenstein, J.L.R. 1997b. Mutations of the homeobox genes *Dlx-1* and *Dlx-2* disrupt the striatal subventricular zone and differentiation of late born striatal neurons. *Neuron* **19:** 27–37.

Arney, K.L. 2003. H19 and Igf2—Enhancing the confusion? *Trends Genet.* **19:** 17–23.

Bejerano, G., Pheasant, M., Makunin, I., Stephen, S., Kent, W.J., Mattick, J.S., and Haussler, D. 2004. Ultraconserved elements in the human genome. *Science* **304:** 1321–1325.

Boffelli, D., Nobrega, M.A., and Rubin, E.M. 2004. Comparative genomics at the vertebrate extremes. *Nat. Rev. Genet.* **5:** 456–465.

Briscoe, J. and Ericson, J. 2001. Specification of neuronal fates in the ventral neural tube. *Curr. Opin. Neurobiol.* **11:** 43–49.

Cassiday, L.A. and Maher, L.J. 2002. Having it both ways: Transcription factors that bind DNA and RNA. *Nucleic Acids Res.* **30:** 4118–4126.

Choi, H.K., Won, L., Roback, J.D., Wainer, B.H., and Heller, A. 1992. Specific modulation of dopamine expression in neuronal hybrid cells by primary cells from different brain regions. *Proc. Natl. Acad. Sci.* **89:** 8943–8947.

Clemens, K.R., Wolf, V., McBryant, S.J., Zhang, P., Liao, X., Wright, P.E., and Gottesfeld, J.M. 1993. Molecular basis for specifc recognition of both RNA and DNA by a zinc finger protein. *Science* **260:** 530–533.

Cobos, I., Calcagnotto, M.E., Vilaythong, A.J., Thwin, M.T., Noebels, J.L., Baraban, S.C., and Rubenstein, J.L. 2005. Mice lacking Dlx1 show subtype-specific loss of interneurons, reduced inhibition and epilepsy. *Nat. Neurosci.* **8:** 1059–1068.

Depew, M.J., Liu, J.K., Long, J.E., Presley, R., Meneses, J.J., Pedersen, R.A., and Rubenstein, J.L. 1999. *Dlx5* regulates regional development of the branchial arches and sensory capsules. *Development* **126:** 3831–3846.

Dignam, J.D., Lebovitz, R.M., and Roeder, R.G. 1983. Accurate transcription initiation by RNA polymerase II in a soluble extract from isolated mammalian nuclei. *Nucleic Acids Res.* **11:** 1475–1489.

Dubnau, J. and Struhl, G. 1996. RNA recognition and translational regulation by a homeodomain protein. *Nature* **379:** 694–699.

Eddy, S. 2001. Non-coding RNA genes and the modern RNA world. *Nat. Rev. Genet.* **2:** 919–929.

———. 2002. Computational genomics of noncoding RNA genes. *Cell* **109:** 137–140.

Engelke, D.R., Ng, S.-Y., Shastry, B.S., and Roeder, R.G. 1980. Specific interaction of a purified transcription factor with an internal control region of 5S RNA genes. *Cell* **19:** 717–728.

Erdmann, V.A., Barciszewska, M.Z., Hochberg, A., deGroot, N., and Barciszewski, J. 2001. Regulatory RNAs. *Cell. Mol. Life Sci.* **58:** 960–977.

Faedo, A., Quinn, J.C., Stoney, P., Long, J.E., Dye, C., Zollo, M., Rubenstein, J.L., Price, D.J., and Bulfone, A. 2004. Identification and characterization of a novel transcript down-regulated in Dlx1/Dlx2 and up-regulated in Pax6 mutant telencephalon. *Dev. Dyn.* **231:** 614–620.

Feng, J., White, B., Tyurina, O.V., Guner, B., Larson, T., Lee, H.Y., Karlstrom, R.O., and Kohtz, J.D. 2004. Synergistic and antagonistic roles of the Sonic hedgehog N- and C-terminal lipids. *Development* **131:** 4357–4370.

Gaiano, N., Kohtz, J.D., Turnbull, D.H., and Fishell, G. 1999. A method for rapid gain-of-function studies in the mouse embryonic nervous system. *Nat. Neurosci.* **2:** 812–819.

Ghanem, N., Jarinova, O., Amores, A., Long, Q., Hatch, G., Park, B.K., Rubenstein, J.L.R., and Ekker, M. 2003. Regulatory roles of conserved intergenic domains in vertebrate *Dlx* bigene clusters. *Genome Res.* **13:** 533–543.

Gilligan, P., Brenner, S., and Venkatesh, B. 2002. Fugu and human sequence comparison identifies novel human genes and conserved non-coding sequences. *Gene* **294:** 35–44.

Graves, L.E., Segal, S., and Goodwin, E.B. 1999. TRA-1 regulates the cellular distribution of the tra-2 mRNA in *C. elegans*. *Nature* **399:** 802–805.

Hark, A.T., Schoenherr, C.J., Katz, D.J., Ingram, R.S., Levorse, J.M., and Tilghman, S.M. 2000. CTCF mediates methylation-sensitive enhancer-blocking activity at the H19/Igf2 locus. *Nature* **405:** 486–489.

Higuchi, R., Fockler, C., Dollinger, G., and Watson, R. 1993. Kinetic PCR analysis: Real-time monitoring of DNA amplification reactions. *Biotechnology (N.Y.)* **11:** 1026–1030.

Horike, S., Cai, S., Miyano, M., Cheng, J.F., and Kohwi-Shigematsu, T. 2005. Loss of silent-chromatin looping and impaired imprinting of DLX5 in Rett syndrome. *Nat. Genet.* **37:** 31–40.

Iler, N., Rowitch, D.H., Echelard, Y., McMahon, A., and Abate-Shen, C. 1995. A single homeodomain binding site confers spatial restriction of Wnt-1 expression in the developing brain. *Mech. Dev.* **53:** 87–96.

Ingham, P.W. and McMahon, A.P. 2001. Hedgehog signaling in animal development: Paradigms and principles. *Genes & Dev.* **15:** 3059–3087.

Kageyama, Y., Mengus, G., Gilfillan, G., Kennedy, H.G., Stuckenholz, C., Kelley, R.L., Becker, P.B., and Kuroda, M.I. 2001. Association and spreading of the *Drosophila* dosage compensation complex from a discrete roX1 chromatin entry site. *EMBO J.* **20:** 2236–2245.

Kelley, R.L. and Kuroda, M. 2000. Noncoding RNA genes in dosage compensation and imprinting. *Cell* **103:** 9–12.

Kinzler, K.W., Ruppert, J.M., Bigner, S.H., and Vogelstein, B. 1988. The GLI gene is a member of the Kruppel family of zinc finger L.G. *Nature* **332:** 371–374.

Kohtz, J.D. and Fishell, G. 2004. Developmental regulation of *EVF-1*, a novel non-coding RNA transcribed upstream of the mouse Dlx6 gene. *Gene Expr. Patterns* **4:** 407–412.

Kohtz, J.D., Baker, D.P., Cortes, G., and Fishell, G. 1998. Regionalization within the mammalian telencephalon is mediated by changes in responsiveness to Shh. *Development* **125:** 5079–5089.

Kohtz, J.D., Lee, H.Y., Gaiano, N., Segal, J.D., Ng, E., Larson, T.A., Baker, D.P., Garber, E.A., Williams, K.P., and Fishell, G. 2001. N-terminal fatty-acylation of Sonic Hedgehog enhances the induction of rodent ventral forebrain neurons. *Development* **128:** 2351–2363.

Lanz, R.B., McKenna, N.J., Onate, S.A., Albrecht, U., Wong, J., Tsai, S.Y., Tsai, M.J., and O'Malley, B. 1999. A steroid receptor coactivator, SRA, functions as an RNA and is present in an SRC-1 complex. *Cell* **97:** 17–27.

Lee, M.P., DeBaun, M.R., Mitsuya, K., Galonek, H.L., Brandenburg, S., Oshimura, M., and Feinberg, A.P. 1999. Loss of imprinting of a paternally expressed transcript with anti-sense orientation to KVLQT1 occurs frequently in Beckwith-Wiedemann syndrome and is independent of insulin-like growth factor II imprinting. *Proc. Natl. Acad. Sci.* **96:** 5203–5208.

Liu, J.K., Ghattas, I., Liu, S., Chen, S., and Rubenstein, J.L. 1997. Dlx genes encode DNA-binding proteins that are expressed in an overlapping and sequential pattern during basal ganglia differentiation. *Dev. Dyn.* **210:** 498–512.

Mansouri, A. 1998. The role of Pax3 and Pax7 in development and cancer. *Crit. Rev. Oncog.* **9:** 141–149.

Martinho, R.G., Kunwar, P.S., Casanova, J., and Lehmann, R. 2004. A noncoding RNA is required for the repression of RNApolII-dependent transcription in primordial germ cells. *Curr. Biol.* **14:** 159–165.

Meller, V.H., Wu, K.H., Roman, G., Kuroda, M.I., and Davis, R.L. 1997. roX1 RNA paints the X chromosome of male *Drosophila* and is regulated by the dosage compensation system. *Cell* **88:** 445–457.

Nemes, J.P., Benzow, K.A., and Koob, M.D. 2000. The SCA8 transcript is an anti-sense RNA to a brain-specific transcript encoding a novel actib-binding protein. *Hum. Mol. Genet.* **9:** 1543–1551.

Nguyen, V.T., Kiss, T., Michels, A.A., and Bensaude, O. 2001. 7SK small nuclear RNA binds to and inhibits the activity of CDK9/cyclin T complexes. *Nature* **414:** 322–325.

Ninomiya, S., Isomura, M., Narahara, K., Seino, Y., and Nakamura, Y. 1996. Isolation of a testis-specific cDNA on chromosome 17q from a region adjacent to the breakpoint of t(12,17) observed in a patient with acampomelic campomelic dysplasia and sex reversal. *Hum. Mol. Genet.* **5:** 69–72.

Olsson, M., Campbell, K., and Turnbull, D.H. 1997. Specification of mouse telencephalic and mid-hindbrain progenitors following heterotopic ultrasound-guided embryonic transplantation. *Neuron* **19:** 761–772.

Panganiban, G. and Rubenstein, J.L. 2002. Developmental functions of the Distal-less/Dlx homeobox genes. *Development* **129:** 4371–4386.

Panganiban, G., Sebring, A., Nagy, L., and Carroll, S. 1995. The development of crustacean limbs and the evolution of arthropods. *Science* **270:** 1363–1366.

Porteus, M.H., Bulfone, A., Ciaranello, R.D., and Rubenstein, J.L.R. 1991. Isolation and characterization of a novel cDNA clone encoding a homeodomain that is developmentally regulated in the ventral forebrain. *Neuron* **7:** 221–229.

Robledo, R.F., Rajan, L., Li, X., and Lufkin, T. 2002. The Dlx5 and Dlx6 homeobox genes are essential for craniofacial, axial, and appendicular skeletal development. *Genes & Dev.* **16:** 1089–1101.

Sabarinadh, C., Subramanian, S., Tripathi, A., and Mishra, R.K. 2004. Extreme conservation of noncoding DNA near HoxD complex of vertebrates. *BMC Genomics* **5:** 75.

Sandelin, A., Bailey, P., Bruce, S., Engstrom, P.G., Klos, J.M., Wasserman, W.W., Ericson, J., and Lenhard, B. 2004. Arrays of ultraconserved non-coding regions span the loci of key developmental genes in vertebrate genomes. *BMC Genomics* **5:** 99.

Santini, S., Boore, J.L., and Meyer, A. 2003. Evolutionary conservation of regulatory elements in vertebrate Hox gene clusters. *Genome Res.* **13:** 1111–1122.

Sasaki, H., Hui, C.C., Nakafuku, M., and Kondoh, H. 1997. A binding site for Gli proteins is essential for the HNF-3b floor plate enhancer activity in transgenics and can respond to Shh in vitro. *Development* **124:** 1313–1322.

Schaeren-Wiemers, N. and Gerfin-Moser, A. 1993. A single protocol to detect transcripts of various types and expression levels in neural tissue and cultured cells; in situ hybridization using digoxigenin-labeled cRNA probes. *Histochemistry* **100:** 431–440.

Schmidt, J.V., Levorse, J.M., and Tilghman, S.M. 1999. Enhancer competition between H19 and Igf2 does not mediate their imprinting. *Proc. Natl. Acad. Sci.* **96:** 9733–9738.

Simeone, A., Acampora, D., Gulisano, M., Stornaiuolo, A., and Boncinelli, E. 1992. Nested expression domains of four homeobox genes in developing rostral brain. *Nature* **358:** 687–690.

Sleutels, F., Zwart, R., and Barlow, D.P. 2002. The non-coding Air RNA is required for silencing autosomal imprinted genes. *Nature* **415:** 810–813.

Snyder, E.Y., Deitcher, D.L., Walsh, C., Arnold-Aldea, S., Hartwieg, E.A., and Cepko, C.L. 1992. Multipotential neural cell lines can engraft and participate in development of mouse cerebellum. *Cell* **68:** 33–51.

Spitz, F., Gonzalez, F., and Duboule, D. 2003. A global control region defines a chromosomal regulatory landscape containing the HoxD cluster. *Cell* **113:** 405–417.

Sutherland, H.F., Wadey, R., McKie, J.M., Taylor, C., Atif, U., Johnstone, K.A., Halford, S., Kim, U.J., Goodship, J., Baldini, A., et al. 1996. Identification of a novel transcript disrupted by a balanced translocation associated with DiGeorge Syndrome. *Am. J. Hum. Genet.* **59:** 23–31.

Tyurina, O.Y., Popova, E., Guner, B., Feng, J., Talbot, W.S., Schier, A.F., Kohtz, J.D., and Karlstrom, R.O. 2005. Zebrafish Gli3 functions as both an activator and a repressor of Hh signaling. *Dev. Biol.* **277:** 537–556.

Wassarman, K.M. and Storz, G. 2000. 6S RNA regulates *E. coli* RNA polymerase activity. *Cell* **101:** 613–623.

Woloshin, P., Song, K., Degnin, C., Killary, A.M., Goldhamer, D.J., Sassoon, D., and Thayer, M.J. 1995. MSX1 inhibits MyoD expression in fibroblast × 10T1/2 cell hybrids. *Cell* **82:** 611–620.

Woolfe, A., Goodson, M., Goode, D.K., Snell, P., McEwen, G.K., Vavouri, T., Smith, S.F., North, P., Callaway, H., Kelly, K., et al. 2005. Highly conserved non-coding sequences are associated with vertebrate development. *PLoS Biol.* **3:** e7.

Wutz, A., Theussl, H.C., Dausman, J., Jaenisch, R., Barlow, D.P., and Wagner, E.F. 2001. Non-imprinted Igf2r expression decreases growth and rescues the Tme mutation in mice. *Development* **128:** 1881–1887.

Yang, Z., Zhu, Q., Luo, K., and Zhou, Q. 2001. The 7SK small nuclear RNA inhibits the CDK9/cyclin T1 kinase to control transcription. *Nature* **414:** 317–322.

Zerucha, T., Stuhmer, T., Hatch, G., Park, B.K., Long, Q., Yu, G., Gambarotta, A., Schultz, J.R., Rubenstein, J.L., and Ekker, M. 2000. A highly conserved enhancer in the Dlx5/Dlx6 intergenic region is the site of cross-regulatory interactions between Dlx genes in the embryonic forebrain. *J. Neurosci.* **20:** 709–721.

Zhang, H., Hu, G., Wang, H., Sciavolino, P., Iler, N., Shen, M.M., and Abate-Shen, C. 1997. Heterodimerization of Msx and Dlx homeoproteins results in functional antagonism. *Mol. Cell. Biol.* **17:** 2920–2932.

Zhou, Q.P., Le, T.N., Qiu, X., Spencer, V., de Melo, J., Du, G., Plews, M., Fonseca, M., Sun, J.M., Davie, J.R., et al. 2004. Identification of a direct Dlx homeodomain target in the developing mouse forebrain and retina by optimization of chromatin immunoprecipitation. *Nucleic Acids Res.* **32:** 884–892.

Zwart, R., Sleutels, F., Wutz, A., Schinkel, A.H., and Barlow, D.P. 2001. Bidirectional action of the Igf2r imprint control element on upstream and downstream imprinted genes. *Genes & Dev.* **15:** 2361–2366.

The *Evf-2* noncoding RNA is transcribed from the Dlx-5/6 ultraconserved region and functions as a Dlx-2 transcriptional coactivator

Jianchi Feng, Chunming Bi, Brian S. Clark, et al.

Genes Dev. 2006, **20:**
Access the most recent version at doi:10.1101/gad.1416106